International Journal of Fatigue 42 (2012) 172–182

Contents lists available at SciVerse ScienceDirect

International Journal of Fatigue

journal homepage: www.elsevier.com/locate/ijfatigue

Prediction of fatigue crack initiation lives at elongated notch roots using short crack concepts

Jaime Tupiassú Pinho de Castro [a,*], Marco Antonio Meggiolaro [a], Antonio Carlos de Oliveira Miranda [b], Hao Wu [c], Abdellatif Imad [d], Noureddine Benseddiq [d]

[a] Mechanical Engineering Department, Pontifical Catholic University of Rio de Janeiro (PUC-Rio), Rio de Janeiro, RJ 22451-900, Brazil
[b] Department of Civil and Ambiental Engineering, University of Brasília, SG-12 Building, Darcy Ribeiro Campus, DF 70910-900, Brazil
[c] The Parading Center of Mechanics Laboratory of Ministry of Education, Tongji University, Shanghai 200092, China
[d] Laboratoire de Mécanique de Lille (CNRS UMR 8107), Université Lille1, Villeneuve D'Ascq, France

ARTICLE INFO

Article history:
Available online 7 November 2011

Keywords:
Notch sensitivity
Short cracks
Non-propagating cracks
Fatigue life prediction
Short crack tolerance

ABSTRACT

Re-initiation lives of fatigue cracks departing from stop-holes roots, previously introduced at the tip of deep cracks on modified SE(T) specimens, have been satisfactorily predicted using their properly calculated notch sensitivity factor q, considering the notch tip stress gradient influence on the fatigue behavior of mechanically short cracks. This is an indispensable detail, since traditional q estimates are only applicable to semi-circular notches, whereas elongated slits can have q values which also depend on their shape, not only on their tip radius. Based on this experimental evidence, a criterion for acceptance of short cracks is proposed.

1. Introduction

The notch sensitivity factor $0 \leqslant q \leqslant 1$ is widely used in structural design to quantify the difference between K_t, the linear elastic stress concentration factor (SCF) of a notch, and K_f, its corresponding fatigue SCF, which quantifies the actual notch effect on the fatigue strength of structural components [1]. The SCF K_t is equal to σ_{max}/σ_n, where σ_{max} is the maximum (linear elastic) stress at the notch root caused by σ_n, and σ_n is the nominal stress that would act at that point if the notch did not affect the stress field around it. The fatigue SCF is usually defined by

$$K_f = 1 + q(K_t - 1) = S_L/S_{L_{ntc}} \tag{1}$$

where S_L and S_{Lntc} are the material fatigue limits (or their fatigue strengths at a convenient very long life) measured on standard (smooth and polished) and on notched test specimens, respectively. But, as the fatigue process depends on two parameters, Eq. (1) can be generalized considering that K_f may depend e.g. on $R = \sigma_{min}/\sigma_{max}$, by writing $K_f(R) = S_L(R)/S_{Lntc}(R)$.

It is well known that q can be associated with the relatively fast generation of tiny non-propagating fatigue cracks at notch roots, see Fig. 1. Indeed, according to Frost et al. [2], early experimental evidence that small non-propagating fatigue cracks are found at notch roots when $S_L/K_t < \sigma_n < S_L/K_f$ goes back as far as 1949. Hence, it is certainly reasonable to expect that such tiny cracks can be used to quantitatively explain why $K_f \leqslant K_t$ and, consequently, that the notch sensitivity can be analytically predictable from the fatigue propagation behavior of short cracks emanating from the notch tip. It is demonstrated below that in fact this can be done using relatively simple but sound mechanical principles, which do not require heuristic arguments, or arbitrary fitting parameters.

To associate the notch sensitivity to the transition between the non-propagating and propagating states of short fatigue cracks, first the influence of stress field gradients around notch roots on their propagation behavior is studied. Knowing that for stress analysis purposes the behavior of notches with depth b and tip radius ρ can be well simulated by elliptical notches with semi-axes b and c and tip radius $\rho = c^2/b$, it is shown that, for any given material, q depends not only on the notch tip radius ρ, but also on its depth b [3,4]. In other words, the crack shape, characterized by its tip radius to depth ρ/c ratio (or by the semi-axes c/b ratio), has a strong influence on its effect on fatigue strength. This means that shallow and elongated notches of same tip radius ρ may have quite different notch sensitivities q.

It is also shown that the material influence on the notch sensitivity depends on its propagation threshold for (long) fatigue cracks $\Delta K_{th}(R)$ and on its fatigue limit for crack initiation from a

* Corresponding author. Tel.: +55 21 3527 1642; fax: +55 21 3527 1665.
E-mail addresses: jtcastro@puc-rio.br (J.T.P. Castro), meggi@puc-rio.br (M.A. Meggiolaro), acmiranda@unb.br (A.C.O. Miranda), wuhao@tongji.edu.cn (H. Wu), abdellatif.imad@polytech-lille.fr (A. Imad), noureddine.benseddiq@univ-lille1.fr (N. Benseddiq).

0142-1123/$ - see front matter © 2011 Elsevier Ltd. All rights reserved.
doi:10.1016/j.ijfatigue.2011.10.010

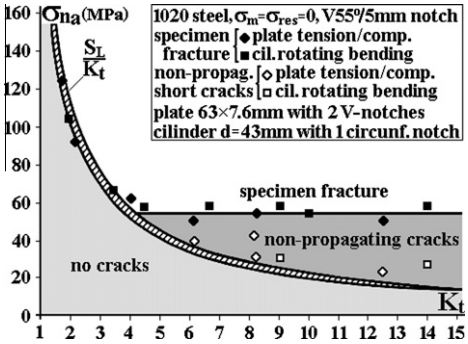

Fig. 1. Classical data showing that non-propagating fatigue cracks are generated at the notch roots if $S_L/K_t < \sigma_n < S_L/K_f$ [2].

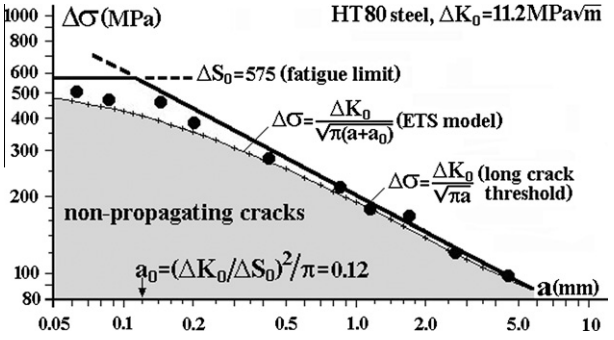

Fig. 2. Kitagawa–Takahashi plot describing the crack size influence on the fatigue propagation of short and long cracks under $R = 0$ in a HT80 steel with $\Delta K_0 = 11.2\ \mathrm{MPa}\sqrt{m}$ and $\Delta S_0 = 575$ MPa [6]: long cracks with $a \gg a_0$ stop when $\Delta\sigma \leqslant \Delta K_0/\sqrt{(\pi a)}$, very short cracks with $a \ll a_0$ stop when $\Delta\sigma \leqslant \Delta S_0$, and the ETS curve predicts crack stop when $\Delta\sigma \leqslant \Delta K_0/\sqrt{\pi(a+a_0)}$.

smooth surface $\Delta S_L(R) = 2S_L(R)$. Note that, from the physical point of view, it is certainly more reasonable to use the stress range and maxima $\Delta\sigma$ and σ_{max} as the crack driving forces, but this old $\Delta\sigma$–R approach has some operational advantages for structural calculations.

The predicted q values are verified by fatigue testing several Al 6082 T6 notched specimens. Finally, it should be noted that "short crack" here means "mechanically short crack" not "microstructurally short crack", since material isotropy is assumed in the modeling. Note, however, that this simplified hypothesis is corroborated by the measured experimental results.

2. The propagation of (mechanically) short fatigue cracks

Short cracks must behave differently from long cracks, since their fatigue crack propagation (FCP) threshold must be smaller than the long crack threshold $\Delta K_{th}(R)$, otherwise the stress range $\Delta\sigma$ required to propagate them would be higher than the material fatigue limit $\Delta S_L(R)$. Indeed, assuming as usual that the FCP process is primarily controlled by the stress intensity factor (SIF) range, for the cases where the SIF range grows as the crack size a increases, $\Delta K \propto \Delta\sigma(\pi a)$, if short cracks with $a \to 0$ had the same $\Delta K_{th}(R)$ threshold of long cracks, their propagation by fatigue would require $\Delta\sigma \to \infty$, a physical non-sense [5].

The crack size influence on the propagation threshold of short fatigue cracks under pulsating loads $\Delta K_{th}(a, R = 0)$ can be satisfactorily modeled using the short crack characteristic size a_0 proposed by El Haddad-Topper-Smith (ETS), which is estimated from $\Delta S_0 = \Delta S_L(R = 0)$ and $\Delta K_0 = \Delta K_{th}(R = 0)$ [6]. This clever trick reproduces well the Kitagawa–Takahashi [7] plot trend, see Fig. 2, using a modified SIF range $\Delta K'$ to describe the fatigue propagation of any crack, short or long,

$$\Delta K' = \Delta\sigma\sqrt{\pi(a + a_0)},\ \text{where}\ a_0 = (1/\pi)(\Delta K_0/\Delta S_0)^2 \tag{2}$$

Using this a_0 trick, it is indeed possible to reproduce the expected limits $\Delta K_{th}(a \to \infty) = \Delta K_0$ and $\Delta\sigma(a \to 0) = \Delta S_0$, see Fig. 2. Knowing that steels typically have $6 < \Delta K_0 < 12\ \mathrm{MPa}\sqrt{m}$, ultimate tensile strength $400 < S_U < 2000$ MPa, and fatigue limit $200 < S_L < 1000$ MPa (because the very clean high-strength steels tend to maintain the $S_L/S_U \cong 0.5$ trend of lower strength steels under fully alternated loads, with $R = -1$); and estimating by Goodman the pulsating ($R = 0$) fatigue limit $\Delta S_0 = 2S_U S_L/(S_U + S_L) \Rightarrow 260 < \Delta S_0 < 1300$ MPa; it can be expected that the maximum range of the ETS short crack characteristic size a_0 for steels is

$$(1/\pi)(\Delta K_{0_{min}}/\Delta S_{0_{max}})^2 \cong 7 < a_0 < 700\ \mu\mathrm{m} \cong (1/\pi)(\Delta K_{0_{max}}/\Delta S_{0_{min}})^2 \tag{3}$$

This a_0 range may be overestimated, since the minimum threshold ΔK_{0min} is not necessarily associated with the maximum fatigue crack initiation limit ΔS_{0max}, nor ΔK_{0max} is always associated with ΔS_{0min}. But it nevertheless justifies the "short crack" denomination used for cracks of a similar small size, and highlights the short crack dependence on the FCP threshold and on the fatigue limit of the material. In other words, it can be expected that cracks up to a few millimeters may still behave as short cracks in some steels, meaning that they may have smaller propagation thresholds than those measured by testing "long" cracks, which have $a \gg a_0$.

Similarly, since the typical strengths of wrought aluminum alloys are $70 < S_U < 600$ MPa, $30 < S_L < 230$ MPa, $40 < \Delta S_0 < 330$ MPa, and $1.2 < \Delta K_0 < 5\ \mathrm{MPa}m$, their maximum a_0 (over)estimated range, and thus their short crack influence scale, is wider than the steels range, $1\ \mu\mathrm{m} < a_0 < 5$ mm.

Since the ETS $\Delta K'$ has been deduced using Griffith's plate SIF, $\Delta K = \Delta\sigma(\pi a)$, Yu et al. [8] and Atzori et al. [9] used the non-dimensional geometry factor $g(a/w)$ of the general SIF expression $\Delta K = \Delta\sigma(\pi a) \cdot g(a/w)$ to deal with other geometries, re-defining

$$\Delta K' = g(a/w) \cdot \Delta\sigma\sqrt{\pi(a + a_0)},\ \text{where}\ a_0 = (1/\pi)[\Delta K_0/(g(a/w) \cdot \Delta S_0)]^2 \tag{4}$$

This expression implies that (under pulsating loads) the tolerable stress range $\Delta\sigma$ tends to the fatigue limit ΔS_0 when $a \to 0$. This is only true when $\Delta\sigma$ is the notch root stress range, instead of the nominal stress. However, the geometry factor $g(a/w)$ found in SIF tables usually includes the notch root SCF, thus use $\Delta\sigma$ instead of $\Delta\sigma_n$ as the notch tip nominal stress range. Hence, a clearer way to define the short crack characteristic size a_0 when it departs from a notch root is to explicitly recognize this practice, separating the geometry factor $g(a/w)$ into two parts: $g(a/w) = \eta \cdot \varphi(a)$, where $\varphi(a)$ describes the stress gradient ahead of the notch tip, which tends to the notch root SCF as the crack length $a \to 0$, whereas η encompasses the remaining terms, such as the free surface correction:

$$\Delta K' = \eta \cdot \varphi(a) \cdot \Delta\sigma\sqrt{\pi(a + a_0)},\ \text{where}\ a_0 = (1/\pi)[\Delta K_0/(\eta \cdot \Delta S_0)]^2 \tag{5}$$

In other words, the first factor $\varphi(a)$ does not appear in this expression for a_0 because for very small cracks the notch root stress range $\varphi(a \to 0) \cdot \Delta\sigma$ should tend to ΔS_0.

Alternatively, from an operational point of view, the short crack problem can be probably more clearly modeled by letting the SIF range ΔK retain its original equation, while the FCP threshold

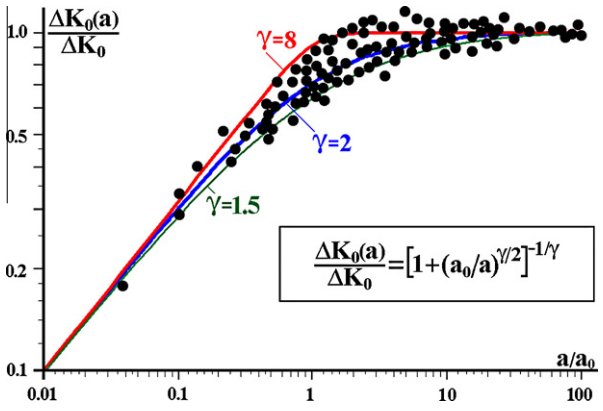

Fig. 3. Ratio between short and long crack propagation thresholds as a function of a/a_0.

expression (under pulsating loads) is modified to become a function of the crack length a, namely $\Delta K_0(a)$, resulting in

$$\Delta K_0(a) = \Delta K_0 \cdot \sqrt{a/(a+a_0)} \tag{6}$$

The El Haddad–Topper–Smith's equation can be seen as one possible asymptotic match between the short and long crack behaviors. Following Bazant's [10] reasoning, a more general equation can be used introducing an adjustable parameter γ to fit experimental data

$$\Delta K_0(a) = \Delta K_0 \cdot [1 + (a_0/a)^{\gamma/2}]^{-1/\gamma} \tag{7}$$

Eqs. (2)–(6) are obtained from Eq. (7) when $\gamma = 2.0$. The bi-linear limit estimate, given in Fig. 2 by $\Delta\sigma(a \leqslant a_0) = \Delta S_0$ for short cracks, and by $\Delta K_0(a \geqslant a_0)$ for long ones, is obtained when $g(a/w) = \eta\cdot\varphi(a) = 1$ and $\gamma \to \infty$. The fitting parameter γ allows this $\Delta K_0(a)$ estimate to better fit short crack propagation data from Tanaka et al. [11] and Livieri and Tovo [12], see Fig. 3. Most data in this figure is bounded by the short crack threshold curves generated using $\gamma = 1.5$ and $\gamma = 8$.

In the following sections, these ideas are first applied to predict the propagation behavior of short cracks emanating from circular holes, and then extended to describe the behavior of cracks which depart from semi-elliptical notches, resulting in improved estimates of the notch sensitivity q and of the largest non-propagating crack size tolerated at such notch tips.

3. The fatigue behavior of short cracks which depart from circular holes

The FCP behavior of short cracks emanating from circular holes in Kirsch (infinite) plates is now evaluated. The SIF of a single crack with length a emanating from a circular hole with radius ρ in a Kirsch plate loaded by a tensile stress range $\Delta\sigma$ is expressed by

$$\Delta K = 1.12 \cdot \varphi(a/\rho) \cdot \Delta\sigma\sqrt{\pi a} \tag{8}$$

where the factor $\varphi(a/\rho) \equiv \varphi(x)$, which describes the hole stress concentration and gradient effects on the SIF, is given (within 1%, [13]) by

$$\varphi(x) = \left(1 + \frac{0.2}{(1+x)} + \frac{0.3}{(1+x)^6}\right) \cdot \left(2 - 2.354\frac{x}{1+x} + 1.2056\left(\frac{x}{1+x}\right)^2 - 0.2211\left(\frac{x}{1+x}\right)^3\right), x \equiv \frac{a}{\rho} \tag{9}$$

Note that, when the crack size a tends to zero, Eq. (8) becomes

$$\lim_{a\to 0} \Delta K = 1.12 \cdot 3 \cdot \Delta\sigma\sqrt{\pi a} \tag{10}$$

as expected, since it combines the solution for an edge crack in a semi-infinite plate with the SCF of a circular Kirsch hole, which has $K_t = \varphi(x = 0) = 3$. Note also that the other limit, for the long cracks with $a \gg a_0$, results in

$$\lim_{a\to\infty} \Delta K = \Delta\sigma\sqrt{\pi a/2} \tag{11}$$

which is the SIF for a long crack with length a in a Griffith (infinite) plate, since the crack tip is so far away from the hole border that it does not suffer anymore the notch influence on its surrounding stress field. Note that the actual crack length is $a + 2\rho$, however, as $a \to \infty$, the ρ value disappears from this equation. Thus, the SIF of a long crack which departs from a Kirsch hole has $\varphi(x \to \infty) = 1/1.12\sqrt{2} \cong 0.63$.

Using Eq. (7) to express the FCP threshold, it can then be stated that any crack departing from a Kirsch hole under pulsating loads will propagate when

$$\Delta K = \eta \cdot \varphi(a/\rho) \cdot \Delta\sigma\sqrt{\pi a} > \Delta K_0(a) = \Delta K_0 \cdot [1 + (a_0/a)^{\gamma/2}]^{-1/\gamma} \tag{12}$$

where $\eta = 1.12$ is the free surface correction. Knowing that the threshold $\Delta K_0(a) \equiv \Delta K_0$ for a long crack, then the crack length parameter a_0 from the above equation is

$$a_0 = (1/\pi)[\Delta K_0/(1.12 \cdot \Delta S_0)]^2 \tag{13}$$

As discussed before, the stress gradient component of the geometry factor $\varphi(a/\rho)$ does not appear in this definition of a_0. The crack propagation criterion given by Eq. (12) can then be restated using two dimensionless functions, one related to the notch stress gradient $\varphi(a/\rho)$, and the other to $g(a/\rho, \Delta S_0/\Delta\sigma, \Delta K_0/\Delta S_0\sqrt{\rho}, \gamma)$ which depends on the crack size, on the fatigue resistances, and on the crack driving force [14], and re-written as

$$\varphi\left(\frac{a}{\rho}\right) > \frac{(\Delta K_0/\Delta S_0\sqrt{\rho}) \cdot (\Delta S_0/\Delta\sigma)}{\left[\left(\eta\sqrt{\pi a/\rho}\right)^{\gamma} + (\Delta K_0/\Delta S_0\sqrt{\rho})^{\gamma}\right]^{1/\gamma}} \equiv g\left(\frac{a}{\rho}, \frac{\Delta S_0}{\Delta\sigma}, \frac{\Delta K_0}{\Delta S_0\sqrt{\rho}}, \gamma\right) \tag{14}$$

In other words, if $x \equiv a/\rho$ and $\kappa \equiv \Delta K_0/\Delta S_0\sqrt{\rho} = \eta \cdot \sqrt{(\pi a_0)^2/\rho}$, a fatigue crack departing from a Kirsch hole under pulsating loads grows whenever $\varphi(x)/g(x, \Delta S_0/\Delta\sigma, \kappa, \gamma) > 1$. Fig. 4 plots some φ/g functions for several fatigue strength to loading stress range ratios $\Delta S_0/\Delta\sigma$ as a function of the normalized crack length x, assuming a notch root radius and short crack characteristic size combination with $\kappa = 1.5$, and a material with $\gamma = 6$ [15].

For high applied stress ranges $\Delta\sigma$, the strength to load $\Delta S_0/\Delta\sigma$ ratio is small, and the corresponding φ/g curve is always higher than 1, meaning that cracks will initiate and propagate from the Kirsch hole border, without stopping during this process. One example of such a case is the upper curve in Fig. 4, which shows the function $\varphi/g_{1.4}$ obtained for $\Delta S_0/\Delta\sigma = 1.4$. On the other hand, small stress ranges $\Delta\sigma$ with load ratios $\Delta S_0/\Delta\sigma \geqslant K_t = 3$ have φ/g functions which are smaller than 1, meaning that no crack will initiate from the Kirsch hole, and that small enough cracks will not propagate from it at such low loads. This is illustrated by curves φ/g_3, associated with the limit case where the local stress range equals the material fatigue strength $\Delta S_0/\Delta\sigma = 3$, and φ/g_4, associated with a still smaller load, $\Delta S_0/\Delta\sigma = 4$.

But three other curves must be analyzed in Fig. 4. The first one crosses the $\varphi/g = 1$ line once, see the $\varphi/g_{2.3}$ curve. This means that such a pulsating intermediate load range can initiate and propagate a fatigue crack from the notch border, until the decreasing (because of the stress gradient ahead of the notch root) $\varphi/g_{2.3}$ ratio reaches 1, where the crack stops. Hence, this $\Delta\sigma = \Delta S_0/2.3$ loading

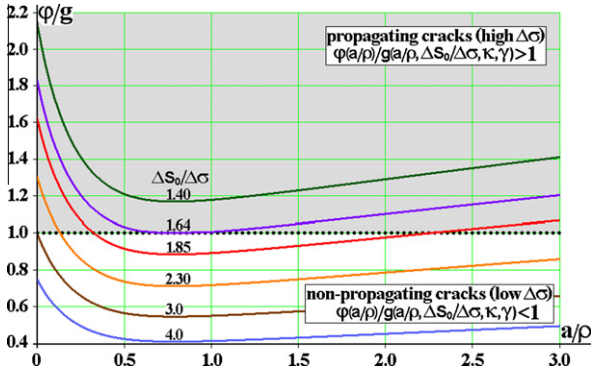

Fig. 4. The fatigue stress concentration factor K_f can be obtained by finding the function φ/g which is tangent to the $\varphi/g = 1$ line, thus in this ($\kappa = 1.5$, $\gamma = 6$) case $K_f = 1.64$.

level generates a non-propagating fatigue crack at this hole border, with a size given by the corresponding a/ρ abscissa.

The second is the $\varphi/g_{1.85}$ curve, which intersects the $\varphi/g = 1$ line twice. This pulsating load level will also generate a fatigue crack at the Kirsch hole border, which will propagate until reaching the maximum size obtained from the abscissa of the first intersection point (on the left), where the crack stops. Moreover, cracks longer than the size defined by the abscissa of that second intersection point will re-start propagating by fatigue under $\Delta\sigma = \Delta S_0/1.85$, until eventually fracturing the Kirsch plate. However, the crack initiated by fatigue under such a pulsating intermediate load range cannot propagate between these two intersection points by fatigue alone (assuming the load range $\Delta\sigma$ and $R = 0$ ratio remain constant.) Hence, it can only grow in this region if helped by a different damage mechanism, such as corrosion or creep, for example.

Note that the FCP behavior of these two curves seems different in Fig. 4, yet they are similar. Indeed, the $\varphi/g_{2.3}$ curve crosses the $\varphi/g = 1$ line twice if the graph is extended to include larger cracks, see Fig. 5, because a sufficiently long crack can always propagate by fatigue under any given (even if small) $\Delta\sigma$ range whenever its SIF range $\Delta K = g(a/w)\cdot\Delta\sigma(\pi a)$ grows with the crack size a, as in this Kirsch plate. In fact, all φ/g curves become higher than 1 for sufficiently large a/ρ values, even those that cannot initiate a crack by fatigue, such as φ/g_4.

Finally, the $\varphi/g_{1.64}$ curve is tangent to the $\varphi/g = 1$ line in Figs. 4 and 5. This means that this stress range $\Delta\sigma = \Delta S_0/1.64$ is the smallest one that can cause crack initiation and propagation (without arrest) from the notch border by fatigue alone. Thus, the fatigue SCF of this Kirsh hole (with $\kappa = \eta\cdot\sqrt{(\pi a_0/\rho)} = 1.5$ and $\gamma = 6$) is, by definition, $K_f = 1.64$. Moreover, the tangency point (between the $\varphi/g_{1.64}$ curve and the $\varphi/g = 1$ line) abscissa gives the largest non-propagating crack size that can arise from it by fatigue alone, $a_{max} = x_{max}\cdot\rho$. For any other γ and $\kappa = \eta\cdot\sqrt{(\pi a_0/\rho)}$ combination, K_f and a_{max} can always be found by solving the system

$$\begin{cases} \varphi/g = 1 \\ \partial(\varphi/g)/\partial x = 0 \end{cases} \Rightarrow \begin{cases} \varphi(x_{\max}) = g(x_{\max}, K_f, \kappa, \gamma) \\ \partial\varphi(x_{\max})/\partial x = \partial g(x_{\max}, K_f, \kappa, \gamma)/\partial x \end{cases} \tag{15}$$

This system can be numerically solved for several combinations of κ and γ, to obtain this notch sensitivity factor q behavior from

$$q(\kappa,\gamma) \equiv (K_f(\kappa,\gamma) - 1)/(K_t - 1) \tag{16}$$

Fixing $\gamma = 6$, the notch sensitivity factor calculated in this way is compared in Fig. 6 to the classical q-curves proposed by Peterson a long time ago (those which are reproduced in most machine elements books), showing that this prediction is indeed reasonable.

Thus, the notch sensitivity q can be calculated using appropriate analytical procedures, without appealing to semi-empirical heuristic arguments, by quantifying how the stress gradient at the notch root affects the short crack propagation, including the material-dependent data fit parameter γ influence on $\Delta K_0(a)$. Moreover, this approach can be easily extended to semi-elliptical notches, which can be modeled in the same way, as shown in the following sections.

Since fatigue is a phenomenon which depends on two driving forces, $\Delta\sigma$ and σ_{max}, before ending this section it must be mentioned that Eqs. (7) and (13) can be easily extended to consider the σ_{max} (here indirectly modeled by the R-ratio) influence in the short crack behavior. First, the short crack characteristic size should be re-defined as

$$a_R = (1/\pi)[\Delta K_R/(1.12\cdot\Delta S_R)]^2 \tag{17}$$

where $\Delta K_R = \Delta K_{th}(a \gg a_R, R)$ is the FCP threshold for long cracks and ΔS_R is the fatigue limit, both measured (or properly estimated) at the desired R-ratio. Likewise, the corresponding short crack FCP threshold should be re-written as

$$\Delta K_R(a) = \Delta K_R\cdot[1 + (a_R/a)^{\gamma/2}]^{-1/\gamma} \tag{18}$$

All these details are important when such models are used to make predictions in real life situations, since they do influence the calculation results. In particular, neglecting the σ_{max} effect on fatigue can lead to severe non-conservative life estimations, thus this potentially dangerous practice cannot be accepted for mechanical design or analysis purposes.

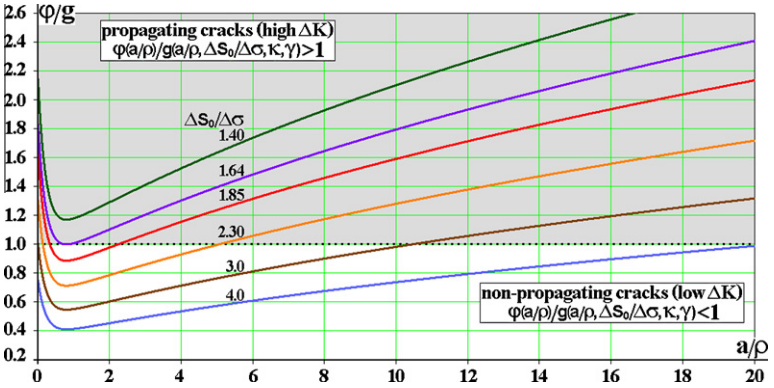

Fig. 5. As after leaving the region affected by the stress gradient near the Kirsh hole border, this crack SIF steadily grows as its size a increases (as usual for far field loaded cracks), any stress range $\Delta\sigma$ can propagate it by fatigue when it is sufficiently long.

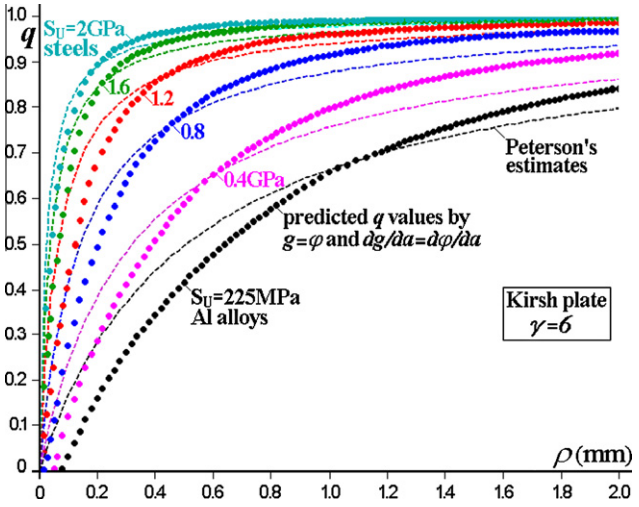

Fig. 6. Notch sensitivity q as a function of the Kirsh hole radius ρ, estimated using the median values of ∂K_0, ∂S_0 and S_U from 450 steels and aluminum alloys, estimated for $\gamma = 6$.

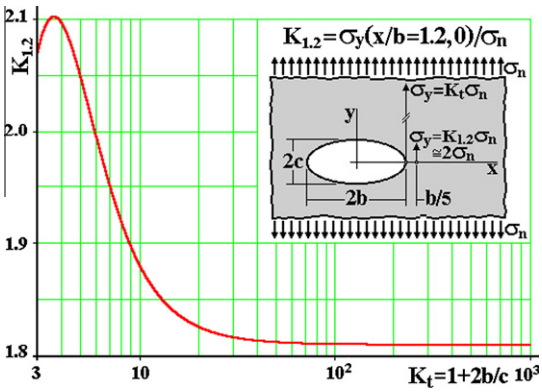

Fig. 7. The ratio $K_{1,2} = \sigma_y(x/b = 1.2, 0)/\sigma_n$ at just $b/5$ ahead of the tip of elliptical Inglis holes is almost independent of its linear elastic SCF $K_t = 1 + 2b/c = 1 + 2\sqrt{(b/\rho)}$.

4. The physical behavior of short cracks which depart from elongated notches

Before jumping into more elaborated mechanics, it is worth to present a simple and unambiguous mechanical explanation to justify why a crack can start from a sharp notch root and propagate for a while before stopping and becoming non-propagating (under fixed loading conditions). This can help to understand why in these cases q must depend not only on ρ and on the material, but also on the notch shape, given by its root radius to depth ratio ρ/b.

A very reasonable estimate for the SIF of a small crack a which departs from the tip of an elliptical notch in an Inglis plate, with semi-axes b and c ($b \gg a$), root radius $\rho = c^2/b$, and with the $2b$ axis centered at the x axis origin, is given by $K_I(a) \cong \sigma_n \cdot \sqrt{(\pi a)} \cdot f_1(a, b, c) \cdot f_2(\textit{free surface})$, where σ_n is the nominal stress (perpendicular to a and b); $f_1(a, b, c) \cong \sigma_y(x)/\sigma_n$; $\sigma_y(x)$ is the stress which acts at the point ($x = b + a$, $y = 0$) in front of the notch root when there is no crack; and $f_2 = 1.12$. The distribution of the $\sigma_y(x = b + a, y = 0)$ stress ahead of the elliptical notch tip is given by [16]:

$$f_1 = \frac{\sigma_y(x, y=0)}{\sigma_n} = 1 + \frac{(b^2 - 2bc)\left(x - \sqrt{x^2 - b^2 + c^2}\right)(x^2 - b^2 + c^2) + bc^2(b - c)x}{(b - c)^2(x^2 - b^2 + c^2)\sqrt{x^2 - b^2 + c^2}} \quad (19)$$

Note that the slender the elliptical notches are, meaning the smaller their semi-axes c/b and tip radius to depth ρ/b ratios are, the higher are their SCF. But higher K_t imply in steeper stress gradients $\partial\sigma_y(x,\ y = 0)/\partial x$ around the notch tip. In fact, the linear elastic SCF induced by any elliptical hole with $b \geqslant c$ drops from $K_t = 1 + 2b/c = 1 + 2\sqrt{(b/\rho)} = \sigma_y(1)/\sigma_n \geqslant 3$ at its tip border to a value $1.82 < K_{1,2} = \sigma_y(1.2)/\sigma_n < 2.11$ at a point just $b/5$ ahead of it, meaning their Saint Venant's controlling distance is associated with their depth b, not with their tip radii ρ, see Fig. 7.

This is the cause for the peculiar growth of short cracks which depart from elongated notch roots. Since the stresses become almost independent on elliptical tip radii after just about $b/5$ from them, the SIF of short cracks departing from slender, high K_t elliptical notches, which in principle should tend to increase with their length $a = x - b$, may instead decrease after they grow for a short while. Indeed, the K_t affected stress gradient effect in the short crack STF $K_I \cong 1.12 \cdot \sigma_n\sqrt{(\pi a)} \cdot f_1$ may decrease sharply due the high stress drop close to the notch tip, overcompensating the crack growth effect, see Fig. 8.

This $K_I(a)$ estimate can be used to evaluate the sizes of non-propagating fatigue cracks tolerable at notch roots, using the short crack FCP behavior. A simple numerical example clarifies this point: if a large steel plate with $S_U = 600$ MPa, $S_L = 200$ MPa and $\Delta K_0 = 9$ MPa·m works under a purely alternated load (stress) range $\Delta\sigma_n = 100$ MPa at R = −1, let's verify if it is possible to change an originally circular $d = 20$ mm central hole by an elliptical one with $2b = 20$ mm (perpendicular to σ_n) and $2c = 2$ mm, without inducing the plate to fail by fatigue.

As $S_L < 0.5S_U/2$, the specified plate fatigue strength probably already considers surface roughness and similar effects. Neglecting the buckling problem, important in thin plates, the circular hole is certainly safe, since it has a safety factor against fatigue crack initiation $\varphi_F = S_L/K_f\sigma_n = 200/150 \cong 1.33$, because this large hole has $K_f \cong K_t = 3$. But the elongated elliptical hole would not be admissible by traditional SN design routines, since it has a very high $K_t = 1 + 2b/c = 21$ and a small tip radius $\rho = c^2/b = 0.1$ mm: its notch sensitivity estimated from the usual Peterson q plot [1] would be $q \cong 0.32 \Rightarrow K_f = 1 + q\cdot(K_t - 1) = 7.33$, thus it would induce a maximum load amplitude $K_f\cdot\sigma_n = 376$ MPa $> S_L$. However, as this K_f value is considerably higher than typical values reported in the literature [15–18], it is worth to re-study this simple problem considering the short crack FCP behavior.

Supposing, as usual, that $\Delta K_{th}(R < 0) \cong \Delta K_0$, and that $S'_L = 0.5S_U$ (S'_L is the material not the plate fatigue limit, as the modifying factors required to estimate the component fatigue limit S_L are not needed for FCP modeling); using ETS to estimate the FCP threshold by $\Delta K_0(a) = K_0/[1 + (a_0/a)]^{-0.5}$, and Goodman to estimate $\Delta S_0 = S_U/1.5$ and $a_0 = (1/\pi)(1.5\Delta K_0/1.12\cdot S_U)^2 \cong 0.13$ mm; then the SIF ranges $\Delta K_I(a)$ for short cracks that depart from the two holes borders are compared to $\Delta K_0(a)$ in Fig. 9.

The SIF $\Delta K_I(a)$ curve for cracks departing from the circular hole remains below the $\Delta K_0(a)$ FCP threshold curve (which considers the short crack behavior) up to $a \cong 1.54$ mm. Thus, if (say) a small surface scratch locally augments the stress range at that hole border up to the point it initiates a tiny crack, this crack would not propagate under this (fixed) $\Delta\sigma_n = 100$ MPa and $R = -1$ load. This confirms its "safe" prediction by traditional SN fatigue design procedures. Only if a crack with $a > 1.54$ mm is introduced at this Kirsch hole border by any other means, it would then be able to propagate by fatigue under those otherwise safe loading conditions.

On the other hand, under these same loading conditions, the $\Delta K_I(a)$ curve for the elliptical hole starts above $\Delta K_0(a)$, thus a crack

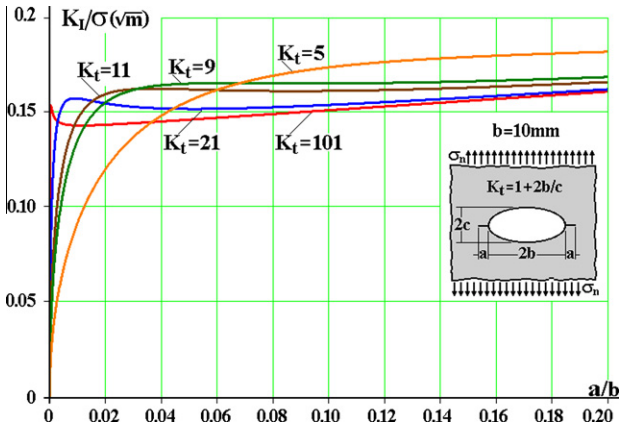

Fig. 8. The estimate $K_I \cong 1.12 \cdot \sigma_n \sqrt{(\pi a)} \cdot f_1(K_t, a)$ for the cracks which depart from the tips of an Inglis elliptical hole with $b = 10$ mm illustrates how the derivative $\partial K_I / \partial a$ may decrease sharply just after the cracks initiate there.

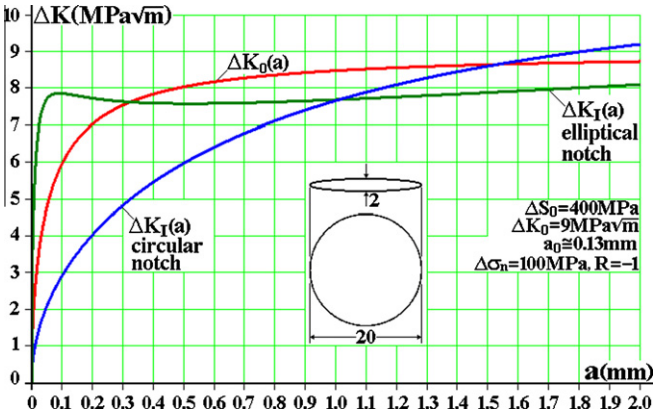

Fig. 9. Cracks do not initiate at the circular hole, which tolerates cracks $a < 1.54$ mm, while the crack which initiates at the elliptical notch tip stops after reaching $a \cong 0.33$ mm.

should initiate at its border, as expected from its high K_t. But as this tiny crack propagates through the high stress gradient ahead of the notch root, it sees rapidly diminishing stresses at its tip during its early growth, which overcompensate the increasing crack size effect on $\Delta K_I(a)$. Eventually this crack SIF becomes smaller than $\Delta K_0(a)$ at $a \cong 0.33$ mm, when it stops and becomes non-propagating (if the nominal $\Delta\sigma_n$ and R loading remain fixed), see Fig. 9. As fatigue failures include crack initiation and growth up to fracture, in this sense both notches could be considered safe for this service loading. However, the non-propagating crack at the elliptical notch tip, a clear evidence of fatigue damage, renders it much less robust than the circular one. For example, a small 10% increment in $\Delta\sigma_n$ could make the crack initiate and propagate from the elliptical notch until the plate fractures, while the circular notch would remain safe, still tolerating a crack $a \cong 1$ mm, as shown in Fig. 10.

These conclusions are quite interesting, but they are based on simple estimates, thus cannot of course be used for analysis purposes. Nevertheless, since these reasonable estimation procedures are based on clear and sound mechanical hypotheses, which do not require heuristic arguments such as ill-defined material-dependent characteristic distances, they do justify the development of the more precise calculations presented in the following section.

5. The analysis of short cracks which depart from elongated notches

The logical reasoning used to model the notch sensitivity of the circular Kirsch hole can now be extended to model elliptical

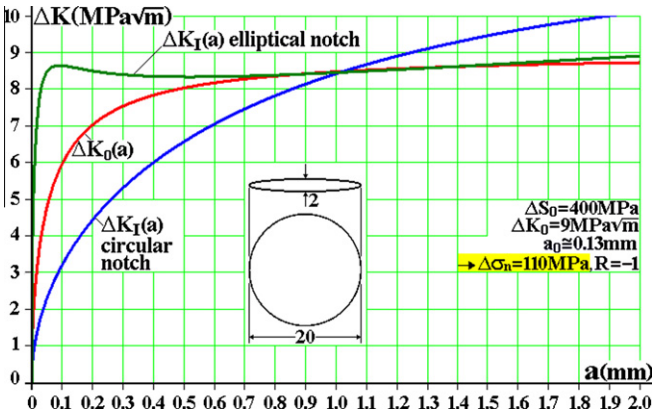

Fig. 10. The circular hole is more robust than the elliptical notch: if the load is increased by just 10%, the crack initiated at the elliptical notch tip does not stop anymore, while the circular hole still tolerates a crack of size $a < \sim 1$ mm departing from its border.

notches, which in turn can be used to model most notches that have the same depth and tip radius. The SIF range of a single crack with length a emanating from a semi-elliptical notch with semi-axes b and c (where b is in the same direction as a) at the edge of a very large plate loaded in mode I can be written as

$$\Delta K_I = \eta \cdot F(a/b, c/b) \cdot \Delta\sigma\sqrt{\pi a} \tag{20}$$

where $\eta = 1.12$ is the free surface correction (FSC), and $F(a/b, c/b)$ is a geometry factor associated with the notch stress concentration, which can be expressed as a function of the dimensionless parameter $s = a/(b + a)$ and of the notch SCF, given by [14]

$$K_t = [1 + 2(b/c)] \cdot \{1 + [0.12/(1 + c/b)^{2.5}]\} \tag{21}$$

To obtain expressions for F, Finite Element (FE) calculations were performed using the Quebra2D program [19,20] considering several cracked semi-elliptical notch configurations. The numerical results, which agreed well with standard solutions [13], were fitted within 3% using empirical equations, resulting in

$$F(a/b, c/b) \equiv f(K_t, s) = K_t\sqrt{[1 - \exp(-sK_t^2)]/sK_t^2}, \quad c \leqslant b \text{ and } s = a/(b + a) \tag{22}$$

$$F'(a/b, c/b) \equiv f'(K_t, s) = K_t[1 - \exp(-K_t^2)]^{-s/2} \times \sqrt{[1 - \exp(-sK_t^2)]/sK_t^2}, \quad c \geq b \tag{23}$$

Fig. 11 shows how well Eq. (22) fits the $F(a/b, c/b)$ points generated by the FE calculations. Similar results are found for Eq. (23) [14].

Note that the SIF expression for cracks departing from semi-elliptical notches include the effect of their K_t (through these F or F' functions) and also retain their η free surface correction, see Eq. (20), since as the parameter $s \to 0$ when $a \to 0$, the maximum stress at their notch tip is given by $\sigma_{max} \to F(0, c/b) \cdot \sigma_n = K_t \cdot \sigma_n$. Thus, just the η factor, but not the $F(a/b, c/b)$ part of K_I, should be considered in the short surface crack characteristic size a_0 definition, as done in Eq. (13).

Note also that the semi-elliptical K_t expression includes a term $[1 + 0.12/(1 + c/b)^{2.5}]$, which could be interpreted as the notch free surface correction. Therefore, when the semi-elliptical notch tends to a crack as $c/b \to 0$, then its SCF $K_t \to 1.12 \cdot 2\sqrt{(b/\rho)}$. This 1.12 factor expresses the free surface correction for the notch, not for the crack. Indeed, when $c/b \to 0$, this 1.12 factor disappears from F, which in this case is given by $F(a/b,\ 0) = 1/\sqrt{s} \Rightarrow \Delta K_I =$

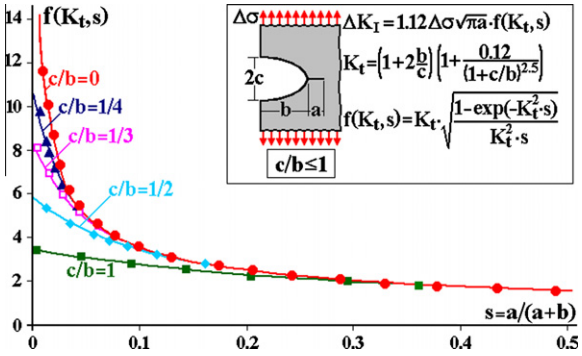

Fig. 11. Finite Element calculations and proposed analytical fit for the geometry factor of semi-elliptical notches with $c \leqslant b$.

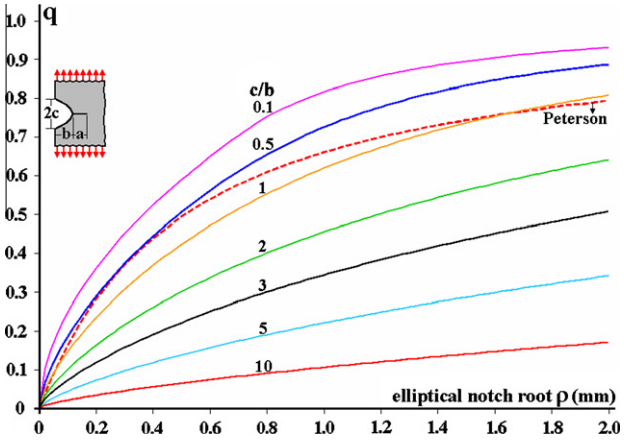

Fig. 12. Notch sensitivity q as a function of the semi-elliptical notch root radius $\rho = c^2/b$ for aluminum alloys having $a_0 = 0.26$ mm ($S_U \cong 225$ MPa and $\Delta K_0 = 2.9$ MPa$\sqrt{m}$.).

$\eta \cdot F \cdot \Delta\sigma \cdot \sqrt{(\pi \cdot a)} = \eta \cdot \Delta\sigma \cdot [\pi \cdot (a+b)]^{0.5}$, as expected, since the resulting crack for $c \to 0$ would have length $a + b$.

Traditional notch sensitivity estimates, based on the fitting of questionable semi-empirical equations to a few experimental data points, assume that q depends only on the notch root ρ and on the material ultimate strength S_U. Thus, similar materials with the same S_U but different ΔK_0 should have identical notch sensitivities, according to those simplistic estimates. The same should occur with shallow and deep elongated notches of identical tip radii. However, whereas well established empirical relations relate the fatigue limit ΔS_0 to tensile strength S_U of many materials, there are no such relations between their FCP threshold ΔK_0 and S_U. Moreover, it is also important to point out that the q estimation for elongated notches by the traditional procedures can generate unrealistic K_f values, as exemplified above. In conclusion, such traditional estimates should not be taken for granted.

The proposed model, on the other hand, is based on the FCP mechanics of short cracks which depart from elliptical notch roots, recognizing that their q values are associated with their tolerance to non-propagating cracks. It shows that their notch sensitivities, besides depending on ρ, ΔS_0, ΔK_0 and γ, are also strongly dependent on their shape, given by their c/b ratio, see Fig. 12. This figure curves are calculated for median aluminum alloy properties: tensile strength $S_U = 225$ MPa, fatigue limit $S_L = 90$ MPa (thus, for pulsating loads by Goodman, $\Delta S_0 = 2S_L S_R/(S_L + S_R) = 129$ MPa), and long crack FCP threshold $\Delta K_0 = 2.9$ MPa$\sqrt{m}$, which give $a_0 = 0.26$ mm, supposing $\gamma = 6$. Similar curves for steels are presented in [14]. Their corresponding Peterson's curve is well approximated by the semi-circular $c/b = 1$ notch, but this curve is ***not*** applicable for much different c/b ratios. Therefore, the proposed predictions indicate that these traditional notch sensitivity estimates should ***not*** be used for elongated notches, a forecast experimentally verified, as discussed in the following section.

6. Experimental verification of the elongated notch sensitivity predictions

Several fatigue tests were carried out on modified SE(T) specimens of thickness $B = 8$ mm and width $W = 80$ mm, to find the number of cycles required to re-initiate the crack after drilling a stop-hole of radius ρ centered at its tip, generating an elongated slit with $b = 27.5$ mm, as detailed in [3,4]. The original objective of those tests was to study the life improvement obtained by the stop-hole repair technique, but these tests can also be used to support the validity of the q calculations. The test specimens were made from an aluminum alloy 6082 T6, with $S_Y = 280$ MPa, $S_U = 327$ MPa, and Young's modulus $E = 68$ GPa. The particularly careful tests were performed at 30 Hz under constant load range at $R = 0.57$, to avoid any eventual crack closure influence on the FCP behavior. The specimens were first pre-cracked until reaching the required crack size. Then they were removed to introduce the stop-holes in a milling machine, using a slight under-size drill precisely centered at their crack tips. Finally, the holes were enlarged to reach their correct size using a reamer. The stop-hole sizes were large enough to remove the plastic zones which followed the previous crack tips.

The fatigue crack re-initiation lives (at the tip of the resulting elongated notch), obtained after repairing the original crack, can be modeled by εN procedures using (i) the Al alloy Coffin–Manson's parameters [21] $\sigma'_f = 485$ MPa, $b = -0.0695$, $\varepsilon'_f = 0.733$ and $c = -0.827$, and Ramberg–Osgood's coefficient and exponent of the cyclic stress–strain curve, $H = 443$ MPa and $h = 0.064$; (ii) the nominal stress range and R-ratio; and finally (iii) the stress concentration factor of the notches generated after repairing the cracks by a stop-hole at their tips, which can be estimated from Eq. (21). Hence, e.g. for a stop-hole radius $\rho = 1$, the resulting SCF is $K_t \cong 12.38$. This slender notch K_t can also be estimated by Inglis, $K_t \cong 1 + 2\sqrt{(a/\rho)} = 11.49$. The SCF calculated by Finite Elements (FE) are $K_t = 11.8$, 8.1, and 7.6 for the 3 stop-hole radii, $\rho = 1$, 2.5, and 3 mm, respectively.

The life improvement introduced by the stop-holes can thus be estimated by calculating the stress and strain maxima and ranges at their root borders by Neuber's rule, and by using them to calculate the crack re-initiation lives by an appropriate $\Delta\varepsilon \times N$ rule, considering the influence of the mean loads. Neglecting this effect could lead to severely non-conservative predictions, as the R-ratio used in the tests was high (and in fact Coffin-Manson predictions are highly non-conservative, thus useless in this case). Figs. 13–15 show that the lives predicted by the elastic version of Morrow's equation (which is an extension of the classical Goodman line) and by the Smith–Watson–Topper (SWT) equation are similar in this case. But it is worth to emphasize that such a similarity cannot be assumed beforehand, since in many other cases these rules can predict very different fatigue lives. Note that these curves are corrected versions of similar curves presented in [4], which lamentably reproduced some imprecise calculations.

The lives predicted for the two larger holes reproduced reasonably well the tests results, see Figs. 13 and 14. But the predictions for the $\rho = 1$ mm hole shown in Fig. 15 are too conservative in comparison to the measured data. Before proceeding, please note that better-than-predicted fatigue lives do not mean that the smaller hole is more efficient than the larger ones. Indeed, as it could be expected, the larger stop-holes are associated with longer fatigue crack re-initiation lives for a given load (in these graphs given by

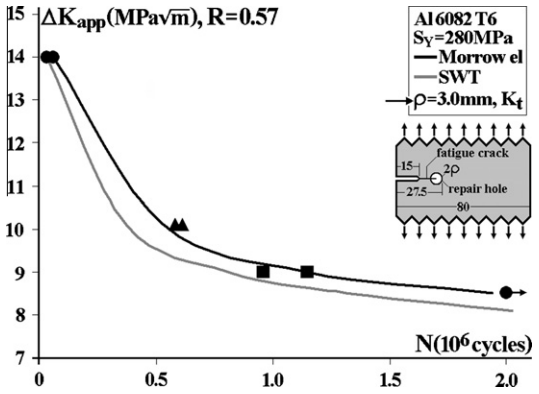

Fig. 13. Predicted and measured fatigue crack re-initiation lives at the $\rho = 3.0$ mm stop-hole borders, using traditional εN procedures: the K_t of the resulting $b = 27.5$ mm elongated slit in Neuber's rule, and Morrow elastic and SWT equations to properly account for the mean or maximum stresses associated with the high $R = 0.57$ loading.

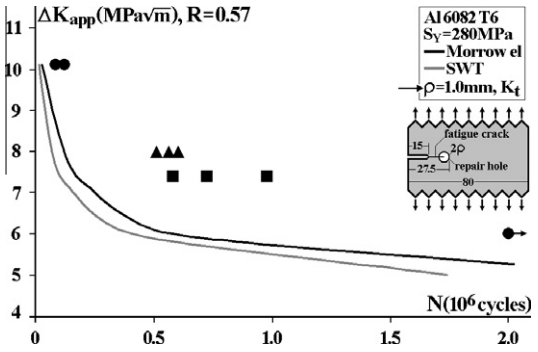

Fig. 15. Measured and similarly predicted fatigue crack re-initiation lives for the $\rho = 1.0$ mm stop-holes (using their K_t and appropriate εN procedures). Note how conservative the predictions in this case are, when compared with the better life predictions obtained for the larger stop-holes.

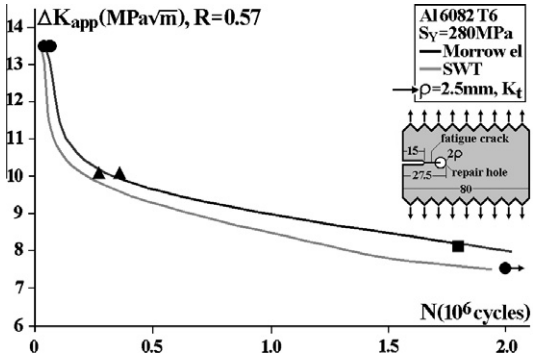

Fig. 14. Measured and similarly predicted fatigue crack re-initiation lives at the $\rho = 2.5$ mm stop-hole borders (using their K_t and appropriate εN procedures).

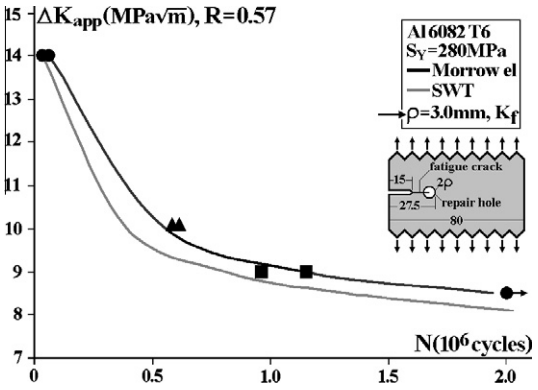

Fig. 16. Predicted and measured fatigue crack re-initiation lives after centering and drilling the stop-holes with radii $\rho = 3.0$ mm at the tip of the crack previously propagated in a SE(T) specimen, using modified εN procedures: the resulting $b = 27.5$ mm elongated slit fatigue SCF K_f estimated using the procedures proposed in this paper (instead of its K_t) in Neuber's rule, and Morrow elastic and SWT equations to properly account for the mean or maximum stresses associated with the high $R = 0.57$ loading. These predictions are similar to those presented in Fig. 13, since these holes $q \cong 1$.

the apparent SIF range ΔK_{app} applied after the repaired specimens were remounted on the fatigue testing machine, calculated treating the resulting $a = 27.5$ mm slits as if they were cracks). From a modeling point of view, the main result obtained from Figs. 13–15 analysis is that εN life predictions made using traditional procedures based on K_t, Neuber, and Morrow or SWT were satisfactory for the larger stop-holes, but severely underestimated the re-initiation lives for the smaller one.

There are few mechanical reasons which can explain the better than expected fatigue lives obtained from the specimens with the smaller stop-holes. One of them would be the presence of significant compressive residual stresses at the $\rho = 1$ mm stop-hole tips. But all the stop-holes were drilled and reamed following identical procedures. Thus, it is reasonable to assume that drilling and reaming processes left the same sub-surface residual stress state around all hole borders, since all hole sizes were large enough to remove the previous crack tip plastic zones, leaving only virgin material ahead of their roots. Moreover, as the bigger stop-hole lives were quite well predicted supposing $\sigma_{res} = 0$, it is difficult to justify why high compressive residual stresses would be present only at the $\rho = 1$ mm stop-hole roots. The same can be said about the surface finish of the stop-holes. However, the smaller stop-holes generate elongated notches with a quite larger K_t than the bigger holes, thus with a much steeper stress gradient near their roots. As discussed above, this effect can significantly affect the growth of short cracks and, consequently, the stop-hole fatigue notch sensitivity, possibly providing a sound mechanical explanation for the measured behavior.

Indeed, when using the properly calculated fatigue SCF K_f instead of K_t with the traditional εN procedures, considering the elongated notch sensitivity q by the method proposed here, all the estimated fatigue crack re-initiation lives reproduce quite well the measured results, see Figs. 16–18. The Al 6082 T6 fatigue limit and fatigue crack propagation threshold under pulsating loads required to calculate K_f are estimated as $\Delta K_0 = 4.8\ \mathrm{MPa}\sqrt{m}$ and $\Delta S_0 = 110$ MPa, following traditional structural design practices. The γ exponent was chosen as $\gamma = 6$, as recommended by [14].

Note that Figs. 15 and 16 present as good predictions as Figs. 13 and 14, since the larger stop-holes notch sensitivity $q \cong 1$, whereas the life predictions for the smaller $\rho = 1$ mm stop-holes presented in Fig. 18 are significantly better than the K_t-based predictions shown in Fig. 15.

Note also that the term "prediction" can in fact be used here, since the curves presented in Figs. 13–18 result from re-initiation life estimations calculated using only mechanical principles and material data obtained from literature [21], without considering any of the measured data points. Thus they are indeed predicted, not data-fitted curves. Moreover, an additional test made ***after*** these calculations predicted that the $\rho = 1$ mm stop-hole could tolerate a $\Delta K_{app} = 7\ \mathrm{MPa}\sqrt{m}$, as indeed it did, see Fig. 18.

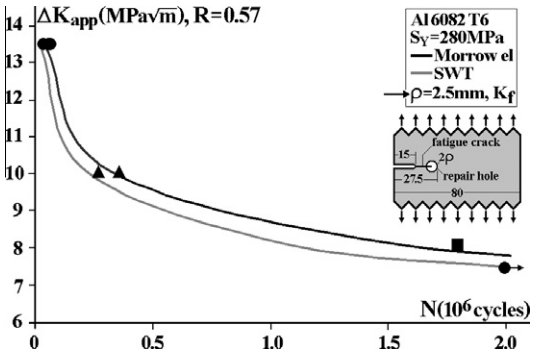

Fig. 17. Measured and similarly predicted fatigue crack re-initiation lives for the $\rho = 2.5$ mm stop-holes (using their properly calculated K_f and appropriate εN procedures). As $q \cong 1$ for these holes too, these predictions are similar to those presented in Fig. 14.

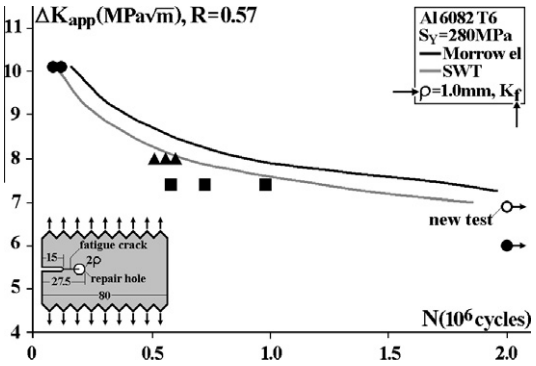

Fig. 18. Measured and similarly predicted fatigue crack re-initiation lives for the $\rho = 1.0$ mm stop-holes (using their properly calculated K_f instead of their K_t in Neuber's rule, and appropriate εN procedures). Note the significant improvement on these life predictions in relation to the K_t-based predictions shown in Fig. 15.

7. An acceptance criterion for short cracks

Based on the encouraging life estimations for these fatigue crack re-initiation data, the reverse path can be followed, assuming the methodology presented here can be used to generate an unambiguous acceptance criterion for small cracks, a potentially much useful tool for practical applications. Most structural components are designed against fatigue crack initiation, using εN or SN procedures which do not recognize cracks. Hence, their "infinite life" predictions may become unreliable when such cracks are introduced by any means, say by an accident during manufacturing or operation, and not quickly detected and properly removed. Large cracks may be easily detected and dealt with, but small cracks may pass unnoticed even in careful inspections, if they are smaller than the detection threshold of the inspection method used to identify them. Thus, structural components designed for very long fatigue lives should be designed to be tolerant to short cracks.

However, this self-evident requirement is still not usually included in fatigue design routines, as most long-life designs just intend to maintain the stress range at the structural component critical point below its fatigue limit, guaranteeing that $\Delta\sigma < S_R/\phi_F$, where ϕ_F is a suitable safety factor. Of course such calculations can become quite involved when designing e.g. against fatigue damage caused by random non-proportional loads, but their philosophy remains the same. Nevertheless, most long-life designs work just fine, which means that they are somehow tolerant to undetectable or to functionally admissible short cracks. But the question "how much tolerant" cannot be answered by SN or εN procedures alone. Such problem can be avoided by adding Eqs. (15) and (16) to the "infinite" life design criterion which, to tolerate a crack of size a in its simplest version, should be written as

$$\Delta\sigma < \Delta K_R/\{\sqrt{\pi a}\cdot g(a/w)\cdot[1+(a_R/a)^{\gamma/2}]^{1/\gamma}\},\ \text{where}$$
$$a_R = (1/\pi)\cdot[\Delta K_R/\eta\Delta S_R]^2 \quad (24)$$

As the fatigue limit $\Delta S_L(R) = \Delta S_R$ already considers the influence of microstructural defects inherent to the structural component material, Eq. (24) complements it considering the component tolerance to cracks. A simple case study can clarify how useful this concept can be, as discussed next.

Due to an unusual manufacturing problem, a batch of a very important component left the factory with small surface cracks, causing some unexpected expensive failures. The task was to estimate the effects of such cracks in the stress range that those steel components could tolerate under uniaxial fatigue loads, knowing that they could be treated as uniaxially loaded strips with 2 mm by 3.4 mm rectangular cross section; that their measured fatigue limit under $R = -1$ is $S_L = 246$ MPa; and their that ultimate strength is $S_U = 990$ MPa. As this $S_L < S_U/2$, it may include some surface roughness effects which should not affect the cracks. But, in the absence of reliable information, the only safe option is to use the measured S_L value to estimate S_R and a_R. Therefore, by Goodman

$$S_R = [S_L S_U(1-R)]/[S_U(1-R)+S_L(1+R)] \quad (25)$$

The mode I stress range $\Delta\sigma$ tolerable by this component when it has a uniaxial surface crack of depth a can thus be expressed by

$$\Delta\sigma < \frac{\Delta K_R/\varphi_F\sqrt{\pi a}}{\left[0.752+2.02\frac{a}{w}+0.37\left(1-\sin\frac{\pi a}{2w}\right)^3\right]\sec\frac{\pi a}{2w}\sqrt{\frac{2w}{\pi a}\tan\frac{\pi a}{2w}}\cdot\left[1+\left(\frac{a_R}{a}\right)^{\gamma/2}\right]^{1/\gamma}} \quad (26)$$

where $w = 3.4$ mm was the component width, and its $g(a/w)$ geometry factor was obtained from [13].

Fig. 19 and 20 plot the maximum tolerable stress ranges (for $\phi_F = 1$) under several R values. As the FCP threshold of these structural components was not available, it had to be estimated by traditional engineering receipts to generate the curves presented in those figures: Hence, their threshold has been assumed within the typical range for steels, $6 < \Delta K_0 < 12$ MPa$\sqrt{\text{m}}$ [15,22], supposing, as usual, that $\Delta K_R \cong \Delta K_0$ for $R < 0$ (since their reported load histories did not include severe underloads). The lower limit FCP threshold estimations used for positive R loads are $\Delta K_{th}(0 < R \leqslant 0.17) = 6$ MPa$\sqrt{\text{m}}$, and $\Delta K_{th}(R > 0.17) = 7\cdot(1 - 0.85R)$ MPa$\sqrt{\text{m}}$. Using $\eta = 1.12$ and $\Delta K_0 = 6$ MPa$\sqrt{\text{m}}$, these components short crack characteristic value is thus estimated as $a_0 = 59$ μm. In this way, Fig. 19 shows that if these components work e.g. under $\Delta\sigma = 286$ MPa and $R = -0.12$, they could tolerate cracks up to $a \cong 105$ μm. Similarly, under $\Delta\sigma = 176$ MPa and $R = 0.44$, they would tolerate cracks up to $a \cong 150$ μm. Fig. 20 uses semi-log coordinates to enhance this component small tolerance to short cracks.

Therefore, this simple (but sensible) model indicates that those (small) components are not too tolerant to 1D surface cracks. However, as this conclusion is based on estimated properties, it is worth to study its sensibility to the assumed property values. Fig. 21 shows the prediction range associated with the typical interval expected for the estimated properties, enhancing how important it is to measure them to obtain less scattered predictions. Such range estimates can be quite useful for designers and quality control engineers, for example they can help decide what to do when a production or operational accident damages the surface of otherwise well-behaved components.

However, this model has some limitations which must be considered. First, it can only be used to describe the behavior of macroscopic short cracks, since it is based in isotropic continuum

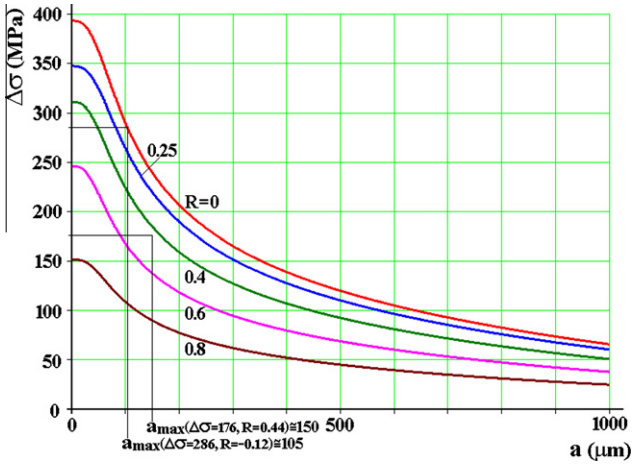

Fig. 19. Effect of a surface crack of size a in the largest stress range $\Delta\sigma_R(a)$ tolerable by a strip of width w = 3.4 mm loaded in mode I, for various R-ratios (it is assumed that it has $\Delta K_0 = 6\ \text{MPa}\sqrt{m}$ and $\gamma = 6$, thus $a_0 = 59$ and $a_{0.8} = 55\ \mu\text{m}$).

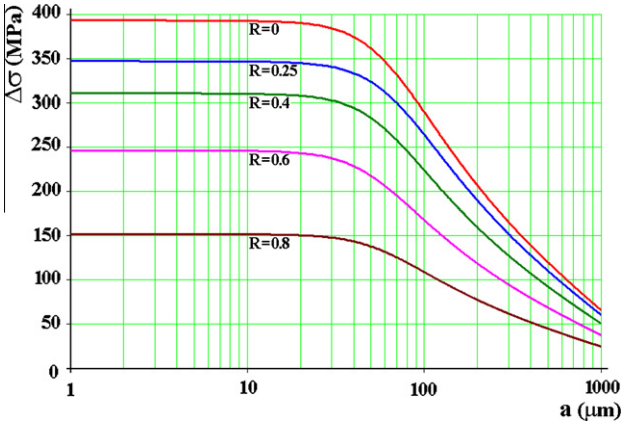

Fig. 20. Similar to Fig. 19, but with semi-log scale to enhance the short crack tolerance of this 3.4 mm wide strip. Note that small cracks with $a < 30\ \mu\text{m}$ have practically no effect in its fatigue resistance.

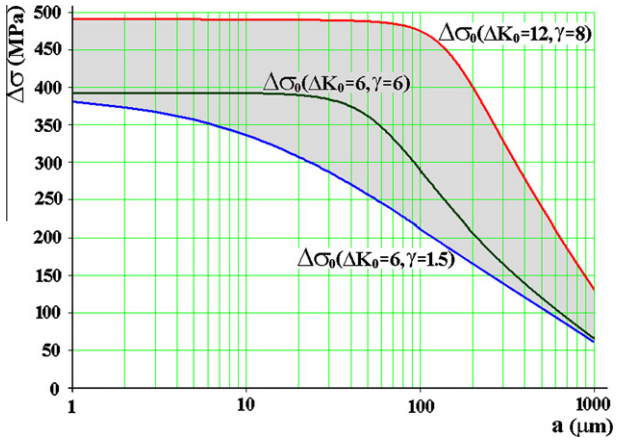

Fig. 21. Typical steel threshold $6 < \Delta K_0 < 12\ \text{MPa}\sqrt{m}$ and γ exponent $1.5 < \gamma < 8$ ranges influence in the largest mode I stress ranges $\Delta\sigma_0$ tolerated by the w = 3.4 mm strip, as a function of the 1D superficial crack size a.

mechanics and uses measured (or estimated) macroscopic material properties. Therefore, it can only be applied to short cracks (compared to a_R) which are large in relation to the characteristic size of the intrinsic material anisotropy (e.g. its grain size). Smaller cracks grow in a size scale where the material is anisotropic and usually inhomogeneous, thus their FCP is also affected at least by microstructural barriers, such as second phase particles or grain boundaries, meaning that their growth under fatigue cannot be assumed independent of such microstructural features. However, as grains and second phase particles cannot be mapped in most practical structural components anyway, such problems, in spite of their potential academic interest, are not really a major barrier from the fatigue design or structural integrity evaluation points of view.

But this model has another limitation which may be more important for practical applications: Eq. (24) assumes that the (short) crack is unidimensional (1D) and grows without changing the original plane of its faces, thus that it can be completely characterized solely by its depth a. But most short cracks are surface or corner cracks, which cannot be completely described in this simplified way. These cracks tend to grow by fatigue at least in two directions, maintaining their original plane when they are loaded under pure mode I conditions. In these cases, they can be modeled as bidimensional (2D) cracks which grow both in depth and width. In reality, both long and short cracks (these meaning cracks not much larger than a_R) only behave as 1D cracks after having cut all the component width to become a through crack, with a more or less straight front which propagates in an approximately uniform way. Thus, Eq. (24) must be adapted to consider this fact.

Therefore, assuming that: (i) the cracks are loaded in pure mode I, under quasi-constant $\Delta\sigma$ and R conditions, with no major overloads; (ii) material properties measured (or estimated) testing 1D specimens may be used to simulate the FCP behavior of 2D cracks; and (iii) 2D surface or corner cracks can be well modeled as having an approximately elliptical front, then their SIF can be described by the classical Newman–Raju equations [15,23]. In this case, it can be expected that the component tolerance to cracks be given by:

$$\Delta\sigma < \begin{cases} \Delta K_R / \{\sqrt{\pi a}\cdot\Phi_a(a,c,w,t)\cdot[1+(a_R/a)^{\gamma/2}]^{1/\gamma}\} \\ \Delta K_R / \{\sqrt{\pi c}\cdot\Phi_c(a,c,w,t)\cdot[1+(a_R/c)^{\gamma/2}]^{1/\gamma}\} \end{cases} \tag{27}$$

For semi-elliptical surface cracks in a plate of thickness t, the SIF in the depth a and width c directions, $K_{I,a} = \sigma\sqrt{(\pi a)}\cdot\Phi_a$ and $K_{I,c} = \sigma\sqrt{(\pi c)}\cdot\Phi_c$, are given by:

$$\begin{cases} K_{I,a} = \sigma\sqrt{\pi a}\cdot\Phi_a = \sigma\sqrt{\pi a}\cdot F\cdot M/\sqrt{Q} \\ K_{I,c} = \sigma\sqrt{\pi a}\cdot\Phi_c = \sigma\sqrt{\pi c}\cdot F\cdot(M/\sqrt{Q})\cdot a/c\cdot G \\ F(c/w,a/t) = \sqrt{\sec[(\pi c/2w)\sqrt{a/t}]}\cdot[1-0.025[(c/w)\sqrt{a/t}]^2 \\ \qquad +0.06[(c/w)\sqrt{a/t}]^4] \\ M = \begin{cases} 1.13-0.09\frac{a}{c}+\left[\frac{0.89}{0.2+a/c}-0.54\right]\frac{a^2}{t^2} \\ +\left[0.5-\frac{1}{0.65+a/c}+14(1-\frac{a}{c})^{24}\right]\frac{a^4}{t^4}, a\leqslant c \\ c/a+0.04(c/a)^2+(c/a)^{4.5}(a/t)^2\left[0.2-0.11(a/t)^2\right], a>c \end{cases} \\ Q = \begin{cases} 1+1.464(a/c)^{1.65}, a\leqslant c \\ 1+1.464(c/a)^{1.65}, a>c \end{cases} \\ G = \begin{cases} 1.1+0.35(a/t)^2, a\leqslant c \\ 1.1+0.35(a/t)^2(c/a), a>c \end{cases} \end{cases} \tag{28}$$

For quarter-elliptical corner cracks, the Φ_a and Φ_c geometry functions are:

$$\begin{cases} \Phi_a = \sec\left(\frac{\pi c}{2w}\sqrt{\frac{a}{t}}\right)\left[0.752 + 2.02\frac{c}{w}\sqrt{\frac{a}{t}} + 0.37\left(1-\sin\left(\frac{\pi c}{2w}\sqrt{\frac{a}{t}}\right)\right)^3\right] \\ \quad \times\sqrt{\frac{2w}{\pi c}\sqrt{\frac{t}{a}}\tan\left(\frac{\pi c}{2w}\sqrt{\frac{a}{t}}\right)} \\ \quad \times\left(1.08 - 0.03\frac{a}{c} + \left(-0.44 + \frac{1.06}{0.3+a/c}\right)\left(\frac{a}{t}\right)^2\right. \\ \quad \left. + \left[-0.5 + 0.25\frac{a}{c} + 14.8\left(1-\frac{a}{c}\right)^{15}\right]\left(\frac{a}{t}\right)^4\right)\frac{1.08+0.15\left(\frac{a}{t}\right)^2}{\sqrt{1+1.464(a/c)^{1.65}}} \\ \Phi_c = \sec\left(\frac{\pi c}{2w}\sqrt{\frac{a}{t}}\right)\left[0.752 + 2.02\frac{c}{w}\sqrt{\frac{a}{t}} + 0.37\left(1-\sin\left(\frac{\pi c}{2w}\sqrt{\frac{a}{t}}\right)\right)^3\right] \\ \quad \times\sqrt{\frac{2w}{\pi c}\sqrt{\frac{t}{a}}\tan\left(\frac{\pi c}{2w}\sqrt{\frac{a}{t}}\right)}\left(1.08 - 0.03\frac{a}{c} + \left(-0.44 + \frac{1.06}{0.3+a/c}\right)\left(\frac{a}{t}\right)^2\right. \\ \quad \left. + \left[-0.5 + 0.25\frac{a}{c} + 14.8\left(1-\frac{a}{c}\right)^{15}\right]\left(\frac{a}{t}\right)^4\right) \\ \quad \times\frac{1.08+0.4\left(\frac{a}{t}\right)^2}{\sqrt{1+1.464(a/c)^{1.65}}} \end{cases} \tag{29}$$

These complicated SIF functions enhance the operational advantage of treating the FCP threshold as a function of the crack size, $\Delta K_{th}(a)$, as claimed above. For structural calculations and mechanical design purposes, it is indeed relatively simple to use either Eqs. (24) and (27) to evaluate the influence of surface cracks on the component fatigue strength. Moreover, it is not too difficult to adapt the 2D equations to include notch effects. However, as this task is not elementary either, it will be treated in a subsequent paper.

8. Conclusions

A generalized El Haddad–Topper–Smith's parameter was used to model the crack size dependence of the threshold stress intensity range for short cracks, as well as the behavior of non-propagating fatigue cracks. This dependence was used to estimate the notch sensitivity factor q of semi-elliptical notches, from studying the propagation behavior of short non-propagating cracks that may initiate from their tips. The predicted notch sensitivities reproduced well the classical Peterson's q estimates for circular holes or approximately semi-circular notches, but it was found that the notch sensitivity of elongated slits has a very strong dependence on the notch aspect ratio, defined by the ratio c/b of the semi-elliptical notch that approximates the slit shape having the same tip radius. These predictions were confirmed by experimental measurements of the re-initiation life of long fatigue cracks repaired by introducing a stop-hole at their tips, using their calculated K_f and appropriate N procedures. Based on this promising performance, a criterion to evaluate the influence of small or large surface cracks in the fatigue resistance was proposed.

Acknowledgements

CNPq, the Brazilian Research Council, has provided research scholarships for the Brazilian authors.

References

[1] Peterson RE. Stress concentration factors. Wiley; 1974.
[2] Frost NE, Marsh KJ, Pook LP. Metal fatigue. Dover; 1999.
[3] Wu H, Castro JTP, Imad A, Meggiolaro MA, Noureddine B. Residual life predictions of repaired fatigue cracks. Solid Mechanics in Brazil 2009, Mattos & Alves ed. ISBN 978-85-85769-43-7. ABCM; 2009.
[4] Wu H, Imad A, Noureddine B, Castro JTP, Meggiolaro MA. On the prediction of the residual fatigue life of cracked structures repaired by the stop-hole method. Int J Fatigue 2010;32:670–7.
[5] Lawson L, Chen EY, Meshii M. Near-threshold fatigue: a review. Int J Fatigue 1999;21:15–34.
[6] El Haddad MH, Topper TH, Smith KN. Prediction of non-propagating cracks. Eng Fract Mech 1979;11:573–84.
[7] Kitagawa H, Takahashi S. Applicability of fracture mechanics to very small crack or cracks in the early stage. Proceedings of the 2nd international conference on mechanical behavior of materials. ASM; 1976.
[8] Yu MT, Duquesnay DL, Topper TH. Notch fatigue behavior of 1045 steel. Int J Fatigue 1988;10:109–16.
[9] Atzori B, Lazzarin P, Meneghetti G. Fracture mechanics and notch sensitivity. Fatigue Fract Eng Mater Struct 2003;26:257–67.
[10] Bazant ZP. Scaling of quasibrittle fracture: asymptotic analysis. Int J Fract 1977;83:19–40.
[11] Tanaka K, Nakai Y, Yamashita M. Fatigue growth threshold of small cracks. Int J Fract 1981;17:519–33.
[12] Livieri P, Tovo R. Fatigue limit evaluation of notches, small cracks and defects: an engineering approach. Fatigue Fract Eng Mater Struct 2004;27:1037–49.
[13] Tada H, Paris PC, Irwin GR. The stress analysis of cracks handbook. Del Research; 1985.
[14] Meggiolaro MA, Miranda ACO, Castro JTP. Short crack threshold estimates to predict notch sensitivity factors in fatigue. Int J Fatigue 2007;29:2022–31.
[15] Castro JTP, Meggiolaro MA. Fatigue – Techniques and Practices for Structural Dimensioning under Real service Loads v.2 (in Portuguese), ISBN 978-1449514709. CreateSpace; 2009.
[16] Schijve J. Fatigue of structures and materials. Kluwer; 2001.
[17] Shigley JE, Mischke CR, Budynas RG. Mechanical engineering design. 7th ed. McGraw-Hill; 2004.
[18] Dowling NE. Mechanical behavior of materials. 3rd ed. Prentice Hall; 2007.
[19] Miranda ACO, Meggiolaro MA, Castro JTP, Martha LF. Fatigue life prediction of complex 2D components under mixed-mode variable loading. Int J Fatigue 2003;25:1157–67.
[20] Miranda ACO, Meggiolaro MA, Martha LF, Castro JTP, Bittencourt TN. Prediction of fatigue life and crack path in generic 2D structural components. Eng Fract Mech 2003;70(10):1259–79.
[21] Borrego LP, Ferreira JM, Pinho da Cruz JM, Costa JM. Evaluation of overload effects on fatigue crack growth and closure. Eng Fract Mech 2003;70(11):1379–97.
[22] Barsom JM, Rolfe ST. Fracture and fatigue control in structures. 3rd ed. ASTM; 1999.
[23] Newman JC, Raju I. Stress-intensity factor equations for cracks in three dimensional finite bodies subjected to tension and Bending Loads. NASA TM-85793; 1984.